



Spatiotemporal variability in otolith elemental fingerprint and the potential to determine deepwater redfish (*Sebastes mentella*) origins and migrations in the Estuary and Gulf of St. Lawrence, Canada

Lola Coussau^{a,b,*}, Dominique Robert^b, Pascal Sirois^a

^a Département des Sciences Fondamentales, Université du Québec à Chicoutimi, Chicoutimi, QC, Canada

^b Institut des Sciences de la Mer de Rimouski, Université du Québec à Rimouski, Rimouski, QC, Canada

ARTICLE INFO

Handled by Maria Teresa Spedicato

Keywords:

Population connectivity
Natal origins
Otolith chemistry
LA-ICP-MS
Sebastes mentella

ABSTRACT

Connectivity processes have major implications in defining the resiliency of fish populations to overexploitation. A preliminary estimate of population exchange rates can be done by identifying the natal origin of adult fish. In this study, otolith elemental fingerprints were used as natural marker of origins and movements of Deepwater redfish (*Sebastes mentella*) in the Gulf of St. Lawrence (GSL). We specifically targeted the strong 2011–2013 cohorts that supported the rapid recovery of the GSL stock after its collapse in the 1990s. Elemental fingerprints were extracted from the core (proxy for larval origin) and edge (proxy for capture location) of otoliths using laser ablation inductively coupled plasma mass spectrometry (LA-ICP-MS). We observed an East to West gradient in the multi-elemental fingerprint of the otolith edge in the GSL, as well as evidence of temporal variation between 2016 and 2018. Cluster analysis of the core fingerprint revealed the existence of two chemically distinct natal sources of variable contribution between the Saguenay Fjord, the western GSL and the eastern GSL. This new insight on the population structure of redfish in the GSL at an ecologically relevant scale constitutes important knowledge for the assessment and sustainable management of a key recovering resource.

1. Introduction

Connectivity processes, consisting of passive and active demographic exchanges among groups of individuals, have major implications for defining the structure, dynamics, and resiliency of fish populations to increasing anthropogenic stressors (Cowen and Sponaugle, 2009; Thorrold et al., 2001). A first assessment of population connectivity consists in determining the natal origin of adult individuals, a characteristic that remains unelucidated for most species (Cowen et al., 2007). Recent advances in tagging and tracking technologies have allowed the reconstruction of fine-scale fish migratory behavior (Block et al., 2005; Cooke et al., 2013). Despite continuous efforts towards increased autonomy and miniaturization of the tags, their use is still limited to relatively large species or older life stages and can only yield data for relatively short periods of time (Secor, 2015). Moreover, unless the tagging experiment is performed in situ (Sigurdsson et al., 2006), the capture and ascent to the surface remains critical for the survival of some deep-sea species that experience barotrauma (Jarvis and Lowe, 2008). As a result, connectivity processes in deep-sea species remain poorly

documented despite a generally high vulnerability to overexploitation (Norse et al., 2012).

Through their continuous growth over the life of the fish, otoliths offer the potential to serve as natural life cycle tracers and constitute a powerful alternative to artificial tags (Campana, 1999). This potential is based on the natural property of otoliths to incorporate chemical elements into the growing calcified structure in proportion to their concentration in the environment (Campana and Neilson, 1985). The metabolically inert nature of otoliths further ensures the preservation of the elemental fingerprint over time (Campana, 1999). Although physiological processes, dietary effects, and/or genetic factors may induce individual variability in elemental incorporation (Clarke et al., 2011; Izzo et al., 2018; Sturrock et al., 2015), it is generally considered that the resulting otolith elemental fingerprint provides a reliable life-time chemical chronology of the environmental conditions experienced by a given individual. Owing to these properties, otoliths have been increasingly used over the past three decades to assess fish migration history, stock structure and population connectivity (Campana, 1999; Elsdon et al., 2008; Kerr, Campana, 2014; Sturrock et al., 2012).

* Corresponding author at: Département des Sciences Fondamentales, Université du Québec à Chicoutimi, Chicoutimi, QC, Canada.

E-mail address: lola.coussau@uqar.ca (L. Coussau).

Appropriate use of otoliths as natural tags in connectivity studies however relies on a thorough assessment of the spatial and temporal variability of the elemental fingerprint and how it is linked with variability in environmental conditions (Elsdon et al., 2008). A temporal change in environmental condition around a stationary fish can be a confounding factor in determining migration patterns that must be detected beforehand (Gillanders, 2002a).

The Deepwater redfish *Sebastes mentella* is a slow-growing and long-lived species (Nedreaas, 1990) historically exploited in the Gulf of St. Lawrence (GSL) along with its congener *Sebastes fasciatus* (Senay et al., 2020). After three decades of low productivity and a moratorium on the fishery since 1995, an unprecedented recruitment event consisting of three consecutive strong year classes (2011, 2012 and 2013) of *S. mentella* resulted in a rapid increase in biomass (Senay et al., 2020). The forthcoming re-opening of the fishery emphasizes the need for better knowledge of the structure and connectivity of the *S. mentella* population in the GSL. The complexity of the genetic structure of redfish populations from the Northwest Atlantic Ocean generated much research interest during the past decade (Benestan et al., 2020; Cadrin et al., 2010; Saha et al., 2017; Valentin et al., 2014). The combined use of genetics and geometric morphometrics identified the Gulf of St. Lawrence-Laurentian channel (GSL-LCH) area as a single biological population (Valentin et al., 2014). The recent use of higher resolution genomic markers on *S. mentella* revealed the structure of the GSL population, where a unique ecotype was identified (Benestan et al., 2020). Beyond the regional information on population structure, genomics however does not provide detailed information on connectivity processes within the population at an ecologically relevant time scale (Thorrold et al., 2002).

The potential for using otolith elemental fingerprints to characterize redfish movements was suggested by Campana et al. (2007), who found evidence of seasonal migrations of *S. mentella* within and outside of the GSL. That study relied on the whole otolith dissolution approach, that provides a fingerprint integrated over the fish's entire life (Elsdon et al., 2008). In order to gain insight on smaller scale redfish life history, the present study was based on laser ablation, an approach differing from otolith dissolution by targeting specific portions of the otolith corresponding to specific life stages. Relying on laser ablation, the aim of the present study was to determine natal sources and estimate connectivity patterns in redfish population from the GSL, largely dominated by the 2011, 2012 and 2013 strong cohorts. First, otolith edge chemistry was used to portray the spatial variation in elemental concentrations in the GSL system and the relation with environmental parameters. The contrast of edge concentration between two sampling years allowed testing the premise of temporal stability of the fingerprint and for possible ontogenic effect. Second, the otolith core fingerprint was analysed through unsupervised Random Forest clustering approach to determine the number of potential origins in *S. mentella* population of the GSL and their respective contribution to post-settled habitats.

2. Materials and methods

2.1. Study area

The Gulf of St. Lawrence is a semi-enclosed sea connecting the Great Lakes basin, the St. Lawrence River and its estuary to the Atlantic Ocean through the Cabot and Belle Isle straits (Fig. 1). The GSL is characterized by multiple bathymetric features, including shelves and deep channels.

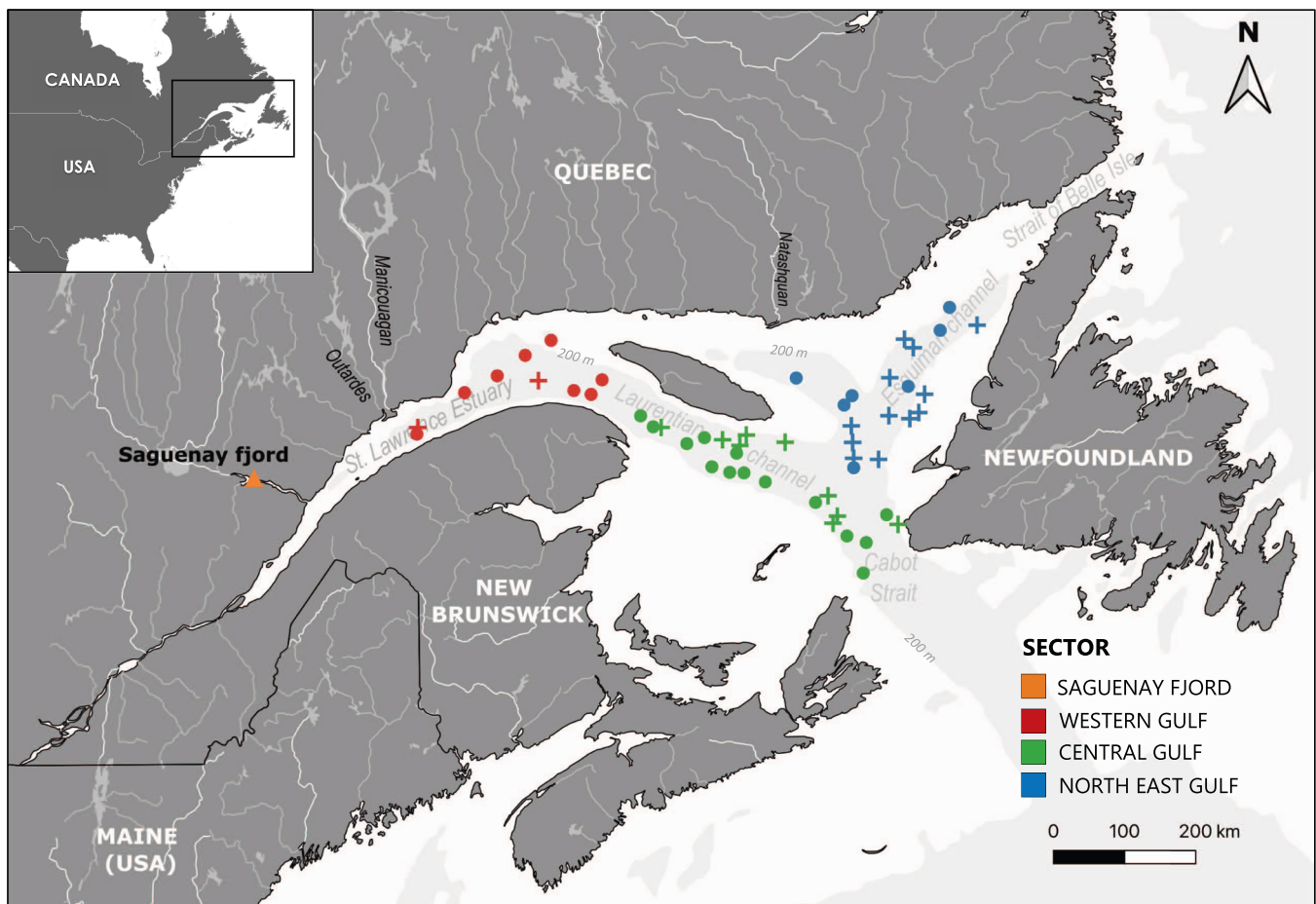


Fig. 1. Sampling locations for redfish juveniles collected in 2016 (+) and 2018 (•) in the Gulf of St. Lawrence and in the Saguenay Fjord (▲).

The Laurentian Channel is the deepest channel of the system (maximum depth of 535 m), extending over 1250 km from the estuary to the continental shelf. Two secondary deep channels branch off from the Laurentian Channel: The Esquiman Channel (maximum depth 335 m) extending towards the Strait of Belle Isle, and the Anticosti Channel (maximum depth 285 m), located North of Anticosti Island. By contrast, the southern part of the GSL consist of a broad and shallow plateau of 80 m deep on average (Koutitonsky and Bugden, 1991) For the purpose of this study, the GSL redfish habitat (waters deeper than 200 m) was divided in three sectors identified by Galbraith et al. (2020) based on physico-chemical characteristics of water masses: The Western Gulf covering the lower estuary up to the mouth of the Saguenay Fjord, the Central Gulf encompassing the deepest part of the Laurentian channel, and the North East Gulf covering the Esquiman and Anticosti channels (Fig. 1). Characterized by an East-West salinity gradient, the waters of the St. Lawrence estuary and gulf exhibit a marked elemental gradient favorable for otolith chemistry studies (Cossa and Poulet, 1978; Morissette and Sirois, 2021). The Saguenay Fjord, a 105 km long and 276 m deep multi-silled glacial valley located at the head of the lower St. Lawrence estuary (Schafer et al., 1990) was also considered in this study as the upstream extreme of the redfish distribution in the system. Current information from genomics, morphometry and natural markers suggests that redfish inhabiting the Saguenay Fjord represent a sink population from the GSL-LCH that is isolated from the GSL individuals (Campana et al., 2007; Sévigny et al., 2009; Sirois et al., 2009; Valentin et al., 2014).

2.2. Sample collection

The study specifically targeted juvenile *S. mentella* from the unprecedented recruitment event in the early 2010's with collection in the GSL in 2016 and 2018 summers, between July and August (Table 1). This was done during the annual multidisciplinary scientific bottom-trawl survey conducted by Fisheries and Ocean Canada (DFO). This annual survey was carried out in the Estuary and northern Gulf of St. Lawrence aboard the CCGS vessel *Teleost* equipped with a Campelen 1800 trawl. Oceanographic data (depth, dissolved oxygen, salinity and temperature) were collected at all fishing stations using a CTD equipped with a dissolved oxygen sensor and deployed on the trawl. Redfish from the Saguenay Fjord were collected by handline from the local ice-fishing activities a few months later during the same fishing season, in January 2019. According to the von Bertalanffy size-at-age model established for redfish in the GSL (Senay et al., 2020), individuals were specifically targeted between 17 and 20 cm fork length (FL) for 2016

sampling and 21–24 FL cm for both 2018 summer sampling in the GSL and winter sampling in the Saguenay Fjord. To obtain samples from the cohort of interest, the same size range was targeted for January sampling in the Saguenay Fjord as individuals are known to exhibit lower growth rate than GSL individuals (Campana et al., 2016). Genetic analysis estimated that 91% of redfish from the targeted strong cohorts belonged to *S. mentella* (Senay et al., 2020). The remaining *S. fasciatus* in the samples were further discriminated through anal fin ray count (Gascon, 2003) which make us confident that only *S. mentella* was considered in the present study.

2.3. Otolith preparation

Sagittal otoliths were extracted, cleaned of organic tissues, triple-rinsed in ultrapure water and stored in polyethylene vials before being dried under a laminar flow flume hood for 24 h. All manipulation tools and storage contents were previously decontaminated for 24 h in 10 % nitric acid (HNO₃), rinsed with ultrapure water and dried under a laminar flow flume hood. The right sagittal otolith was embedded in epoxy resin (in a 4:1 ratio of Miapoxy 100 and Miapoxy 95, Freeman, OH, USA) and transversely sectioned (600 µm thick section on average) through the core of the otolith with a slow-speed diamond-bladed saw (IsoMet saw; Buehler, IL, USA) using ultrapure water as coolant and lubricant. Transverse sections were polished with 3 grades of aluminum oxide polishing (1200-µm grade, 3 MTM) and lapping films (1- and 5-µm grade, 3 MTM) and lubricated with ultrapure water. Polished sections were mounted on petrographic slides with thermoplastic glue (CrystalbondTM 509; AremcoTM products, NY, USA), after which they were sonicated in ultrapure water for 5 min, triple-rinsed and dried under a laminar flow fume hood for 24 h.

2.4. Trace element analysis

Otolith samples were analysed in random order. Two ablation transects per otolith (60 s duration each) were performed through the core to obtain the natal elemental fingerprint, and through the outermost 35 µm of the otolith ventral edge (corresponding to ca. the last weeks of life) to get the elemental fingerprint at the capture location. Otolith trace elemental concentrations were determined in LabMaTer (University of Quebec at Chicoutimi) using laser ablation inductively coupled plasma mass spectrometry [LA-ICP-MS; Resolution M-50 Excimer (193 nm) Arf laser (Australian Scientific Instruments)] equipped with a double volume cell S-155 (Laurin Technican) and coupled with an Agilent 7900x qICP-MS. Laser spot energy density was set to 4 J·cm⁻² with 30 Hz

Table 1

Number of individuals per sector, sampling year, and per ablation site. Total per categories are indicated in bold.

Ablation	Sampling year	Sampling sector				Total
		WESTERN GULF	CENTRAL GULF	NORTH EAST GULF	SAGUENAY	
Edge	2016	22	65	72	0	159
	2018	39	100	58	0	197
	2019	0	0	0	11	11
		61	165	130	11	367
Core	2016	20	64	70	0	154
	2018	39	97	56	0	192
	2019	0	0	0	11	11
		59	161	126	11	357

frequency, 33 μm beam diameter, and 5 $\mu\text{m}\cdot\text{s}^{-1}$ ablation rate. The ablated material was carried into the ICP-MS by an Argon–Helium gas mix at a rate of 0.8 $\text{L}\cdot\text{min}^{-1}$ for Argon and 350 $\text{mL}\cdot\text{min}^{-1}$ for Helium, and 2 $\text{mL}\cdot\text{min}^{-1}$ for Nitrogen also added to the mixture. A 20 s gas blank acquisition preceded each transect, for a total acquisition time of 180 s per otolith. Four reference materials (SRM-610 and SRM-612 obtained from NIST, MD, USA; GSE-1, GP4-A and MACS-3 obtained from USGS, CO, USA, see Lazartigues et al., 2014 for precision on the reference materials) were analyzed at the beginning and the end of each LA-ICP-MS session, and after processing 6 otoliths (roughly every 30 min). A total of 38 elements and isotopes were measured: ^7Li , ^{11}B , ^{23}Na , ^{24}Mg , ^{25}Mg , ^{27}Al , ^{29}Si , ^{31}P , ^{34}S , ^{39}K , ^{42}Ca , ^{43}Ca , ^{44}Ca , ^{55}Mn , ^{56}Fe , ^{57}Fe , ^{59}Co , ^{60}Ni , ^{61}Ni , ^{63}Cu , ^{64}Zn , ^{65}Cu , ^{66}Zn , ^{69}Ga , ^{85}Rb , ^{86}Sr , ^{87}Sr , ^{88}Sr , ^{111}Cd , ^{114}Cd , ^{118}Sn , ^{119}Sn , ^{120}Sn , ^{136}Ba , ^{137}Ba , ^{138}Ba , ^{202}Hg , and ^{208}Pb . Data reduction was carried out using the Iolite package for Igor Pro software from Wavemetrics Incorporated (Paton et al., 2011). In the procedure, calcium (^{44}Ca) was used as an internal standard and assumed to compose 38.02% of the otolith mass (Campana, 1999) and calibration was performed using NIST SRM-610 reference material (Chen et al., 2011). Only samples considered stable in their calcium concentration were retained for further analysis, ^{43}Ca profiles were checked for the presence of irregularities in the otolith matrix. Trace elemental concentrations were expressed as parts per million (ppm). The high stability of the calcium concentration in otoliths and the absence of direct comparison with water concentration did not justify the calculation of element:Ca ratios.

2.5. Age estimation

Following LA-ICP-MS analysis, age estimations were done on the same otolith transverse section photographed under transmitted light using a Leica® M125C stereomicroscope coupled with the Leica MC 170 HD-A microscope camera. Age validation and longevity has been previously verified in the genus *Sebastes* (Campana et al., 1990 for *Sebastes mentella* from the Scotian Shelf, Leaman and Nagtegaal, 1987 for *Sebastes flavidus* from Canadian West coast, Mayo et al., 1981 for *Sebastes marinus* from the Gulf of Maine-Georges Bank region). Annual increments were defined as the succession of a translucent and an opaque growth zone. Reading marks were placed on the border of the opaque zone and the increment widths were measured from otolith core to the edge of the otolith on the ventral axis (Fig. 2) using the ImageJ 1.52a software (<http://imagej.nih.gov/>), and the ObjectJ plugin 1.04x (<https://sil.fnwi.uva.nl/bcb/objectj/examples/TreeRings/TreeRings-9.htm>). Two independent readings were performed, the second after image sharpening applying the unsharp mask filter implemented in Adobe Photoshop CS2 (<http://www.adobe.com/products/photoshop.html>). The test of symmetry ($p = 0.8628$) indicated that there were no systematic differences in age determination between the two readings, the age assigned from the filtered photo was selected for further analysis.

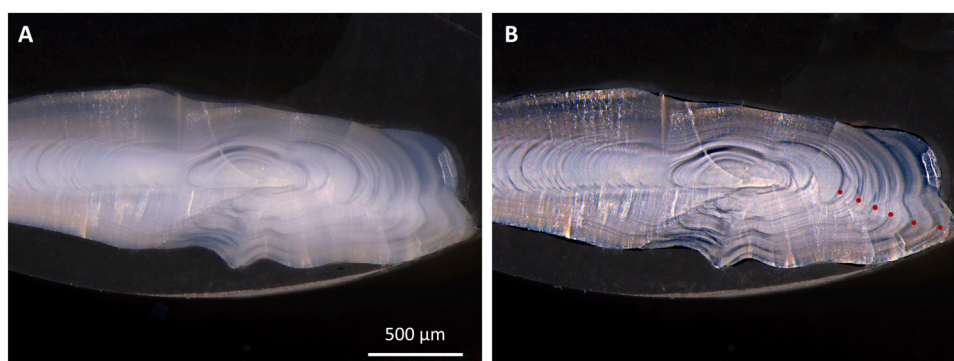


Fig. 2. Photographs of *S. mentella* otoliths section (A) without filter and (B) with unsharp mask filter implemented in Adobe Photoshop and age 6 reading marks.

2.6. Data analyses

Several chemical elements and isotopes were excluded before statistical analysis as they yielded values below the limit of detection (LOD; calculated as three times the standard deviation of the gas blank divided by the sensitivity of the instrument signal) associated with LA-ICP-MS technique, or due to suspected interferences and contamination. Five elements, Li, Na, Mn, Sr, and Ba were ultimately retained, with Mn only detected in otolith core. These five elements were also considered informative in an earlier study tracking redfish movement in the GSL (Campana et al., 2007). All statistical analyses were performed on $\ln(x + 1)$ transformed data to meet the assumptions of normality and homoscedasticity of residuals. Multivariate outliers for otolith core and edge analysis respectively were excluded once identified by Mahalanobis Distance tests.

2.6.1. Spatial and temporal variations in otolith fingerprint

The effect of age on otolith edge elemental concentrations was tested with analysis of variance (ANOVA) followed by Tukey's HSD tests. Linear regressions were performed to test the relation between the elemental concentrations from otolith edge (corresponding to the capture location) and the environmental parameters measured at the time and location of the fish sampling. Regressions were carried out using the 53 stations sampled across all sectors during the two years, based on mean elemental concentrations measured among individuals captured at each station (2–12 individuals per station). Spatial (among-sector) and temporal (between-year) variability in environmental parameters in the GSL was tested with ANOVA. Then, pairwise comparisons were conducted by Tukey's HSD tests. Spatial, temporal, and between cohort variation in otolith edge fingerprint as well as the interaction factors were tested with MANOVA for multi-elemental fingerprint and ANOVA for single element analysis. The significance of the MANOVA was tested with the Pillai trace statistic as it is the most robust to deviations from multivariate normality (Quinn and Keough, 2002). ANOVA for single element were followed up by a Tukey's HSD multiple comparison test to determine which sector, year, or combination of the two, in a case of a significant interaction, differed. Stepwise quadratic discriminant function analysis (QDFA) based on Li, Na, Sr, and Ba concentrations in otolith edges was used to determine elements contributing the most to spatial differences in elemental fingerprint. For each of the 2016 and 2018 years of sampling, the first two canonical functions of the QDFAs were plotted against each other to visually assess the spatial differences in the elemental fingerprint (Kerr and Campana, 2014). Classification to collection success from the QDFAs were presented separately for 2016 and 2018.

2.6.2. Natal origins

Clustering analysis was performed on the otolith core elemental fingerprint to gain insights into the number of natal sources contributing to the GSL and Saguenay Fjord juvenile samples. As a first step, one-way

MANOVA was used to assess whether there was no difference in otolith core multi-elemental fingerprint between the three identified cohorts. Significant differences in otolith core fingerprint were then assumed to represent spatially distinct natal origins. Thereafter, the random forest (RF) clustering method proposed by Breiman and Cutler (2003) was applied in an unsupervised way, a technique developed by Shi and Horvath (2006). This unsupervised clustering method has proven to be powerful for natal origin investigations when knowledge of larval source location is lacking (Artetxe-Arrate et al., 2019; Gibb et al., 2017; Pan et al., 2020; Régnier et al., 2017; Wright et al., 2018a,b). Unsupervised RF clustering consists in training the RF classifier to discriminate between original data and a synthetic dataset created through random sampling from the product of empirical marginal distributions of the variables (here the chemical elements) by bootstrapping of each variable separately. The RF proximity matrix defined by the frequency at which two individuals from the original dataset end up in the same terminal node of the trees is extracted and converted to a dissimilarity matrix. The dissimilarity matrix is then used as an input in partitioning around medoid (PAM) clustering (Kaufman and Rousseeuw, 1990) to group the juvenile redfish into RF-identified clusters. The appropriate number of clusters was determined using the cValid R package (Brock et al., 2008), allowing multiple combinations of validation measures to be tested while varying the number of clusters.

3. Results

3.1. Environmental parameters and otolith edge elemental concentrations

Significant variability was observed between the three GSL sectors in salinity (ANOVA, $p < 0.0035$) dissolved oxygen (ANOVA, $p < 0.0014$) and sampling depth (ANOVA, $p < 0.0001$). Tukey's HSD test revealed that the statistically higher salinity levels coincided with the higher sampling depths (Fig. 3). Dissolved oxygen concentrations were

statistically higher in the Central and North East Gulf sectors compared to the West of the GSL in both years. For temperature, the standard deviation was relatively large within the North East Gulf sectors, which explains why no significant spatial difference was found. Significant between-year variability was observed in dissolved oxygen concentrations with higher levels in 2016 than in 2018 (ANOVA, $p < 0.01$). Sampling depth tended to be higher in 2018, with warmer and saltier water masses compared to 2016. Linear regressions showed significant positive relations between Sr in otolith edge and water temperature and salinity, and by extension with depth. A positive relationship was found between Ba and dissolved oxygen (Table 2).

3.2. Spatial and temporal variation in otolith elemental fingerprint

MANOVA suggested the existence of both spatial and temporal variation in otolith edge chemistry, with a significant interaction found between the two factors (Table 3). The multi-elemental fingerprint did not vary significantly among individuals from different cohorts. ANOVA performed on a single element revealed that the interaction term was significant for Sr and Ba. Considering the interaction effect, post-hoc Tukey's HSD test showed that between-year variation in Sr and Ba concentrations was mainly observed in the North East Gulf sector, where overall higher concentrations in Sr and lower concentrations in Ba were measured in 2018 compared to 2016. In contrast, Ba and Sr concentrations remained relatively stable over time in the Western Gulf and Central Gulf sectors (Fig. 4). An increasing West to East gradient was observed in Sr concentrations in 2018, while there was a decreasing one in 2016. For Ba, an increasing gradient toward the East was found from the Western Gulf to the North East Gulf sector for both years. ANOVA showed that only significant between-year differences were found for Li (Year: $F = 27.73$, $df = 1$, $p < .0001$), with overall higher concentrations in 2016 compared to 2018. Na concentrations in otolith edge did not statistically vary spatially or inter-annually between the three GSL

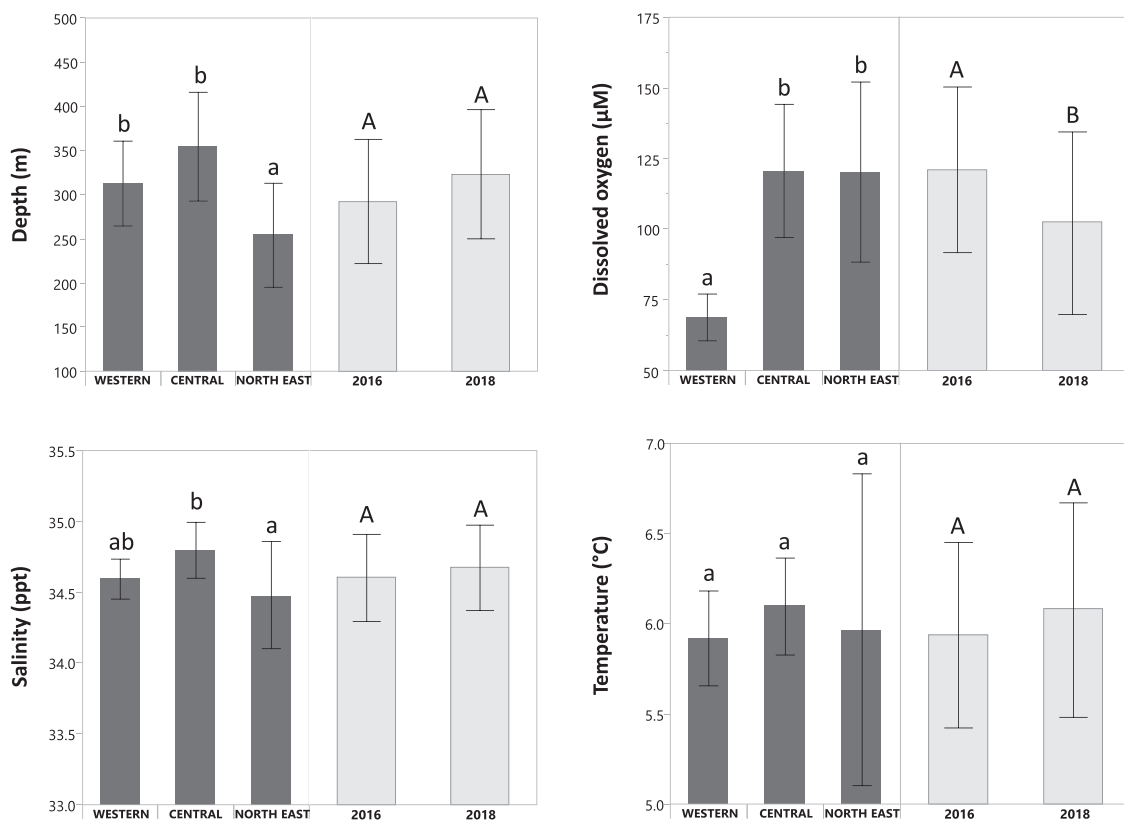


Fig. 3. Mean and standard deviations for environmental parameters measured at the three GSL sectors for 2016 and 2018 sampling years. Capital letters represents significant between-year differences from Tukey HSD and lower-case letter significant spatial differences.

Table 2

Summary of linear regressions between otolith edge elemental concentrations and environmental factors. Significant relationships (p-value <0.05) are indicated in bold.

Factor	Element	Slope	df	R ²	F	p
Temperature	Li	-0.4075	50	0.0091	0.46	0.5010
	Na	-131.94	50	0.0423	2.21	0.1434
	Sr	197.10	50	0.1008	5.60	0.0218
	Ba	1.1047	50	0.0203	1.04	0.3134
Salinity	Li	-0.2908	50	0.0014	0.07	0.7955
	Na	-279.90	50	0.0557	2.95	0.0921
	Sr	470.60	50	0.1679	10.09	0.0026
	Ba	2.1080	50	0.0216	1.11	0.2980
Dissolved oxygen	Li	0.0022	50	0.0009	0.04	0.8335
	Na	1.6910	50	0.0229	1.17	0.2839
	Sr	1.4140	50	0.0171	0.87	0.3552
	Ba	0.0477	50	0.1251	7.15	0.0101
Depth	Li	-0.0021	50	0.0040	0.20	0.6554
	Na	-1.1170	50	0.0515	2.72	0.1055
	Sr	1.8920	50	0.1578	9.37	0.0035
	Ba	0.0011	50	0.0003	0.02	0.8988

Table 3

Results of full factorial models for a) MANOVA and b) ANOVA) examining temporal (Year), spatial (Sector), cohort effect on variation in elemental concentrations measured in otolith edge of redfish from the GSL. Significant relationships (p-value <0.05) are indicated in bold.

a) MANOVA				
Source	Pillai Trace	df	F	p-value
Year	0.24	1	26.85	< .0001
Sector	0.13	2	6.03	< .0001
Cohort	0.04	2	1.74	0.0860
Year x Sector	0.14	2	3.84	< .0001
Cohort x Year	0.04	2	1.88	0.0603
Sector x Cohort	0.35	4	0.77	0.7205
b) ANOVA				
	Source	df	F	p-value
Li	Year	1	27.73	< .0001
	Sector	2	0.52	0.594
	Year x Sector	2	0.28	0.757
Na	Year	1	0.50	0.481
	Sector	2	0.18	0.834
	Year x Sector	2	0.94	0.391
Sr	Year	1	6.94	0.009
	Sector	2	1.10	0.333
	Year x Sector	2	6.56	0.002
Ba	Year	1	41.69	< .0001
	Sector	2	30.57	< .0001
	Year x Sector	2	5.38	0.050

sectors. Note that the Saguenay Fjord was not included in the ANOVAs for spatio-temporal investigation in elemental concentrations but Sr and Li in otoliths appeared to be lower than all Gulf sectors although Na concentrations seemed higher. As MANOVA showed temporal variation

in elemental fingerprint, QDFAs were performed separately for 2016 and 2018 sampling. For both years, the stepwise analysis selected 4 chemical elements for discriminating the sampling sectors. For both years the total variance was mostly explained by the first function (91.5 % for 2016 and 62.8.7 % for 2018; Fig. 5). For 2016, Sr and Ba mainly contributed to the first canonical function and Li and Na to the second one. For 2018, Li, Na, and Sr mainly contributed to the first function and Ba to the second. In 2016, Sr and Ba appeared to be the main elements that distinguished individuals from the three GSL sectors. A decrease in Sr and an increase in Ba concentrations in redfish otoliths was observed from the Western Gulf to the North East Gulf sectors. For 2018, it was essentially Ba responsible for the West to East sector distinction. With a 100 % classification success, the Saguenay Fjord was clearly distinguished from GSL sectors based on the multi-elemental fingerprint (Table 4). The Western Gulf sector was also well separated from the others, with a QDFA classification success of 96 % for 2016 and 79 % for 2018. The Central and North East Gulf sectors were more difficult to distinguish from each other as shown by the overlap in the elemental fingerprints in the QDFA biplot and the weak to moderate classification successes.

3.3. Age effect

ANOVA revealed that Ba and Li concentrations in otolith edges varied significantly with fish age (Ba, $F = 9.942$, $P < 0.0001$; Li, $F = 7.089$, $P < 0.0001$). Tukey's HSD test showed that concentrations of Li and Ba elements were lower in older individuals (Supplementary Fig. S1).

3.4. Natal origins

MANOVA showed no difference in core chemistry among the 2011, 2012 and 2013 cohorts (Pillai's trace statistic = 0.0414, $F = 1.48$, $df = 2$, $p = 0.1412$). RF clustering on otolith core Ba, Sr, Na, Mn, and Li concentrations, here ordered by variable of importance, identified two chemically distinct natal sources (MANOVA, Pillai's trace statistic = 0.4915, $F = 67.86$, $df = 1$, $p < 0.0001$). Source 1 was characterized by lower concentration of Mn and elevated concentration of Li, Na, Sr and Ba compared to source 2 (Fig. 6). Both sources were detected

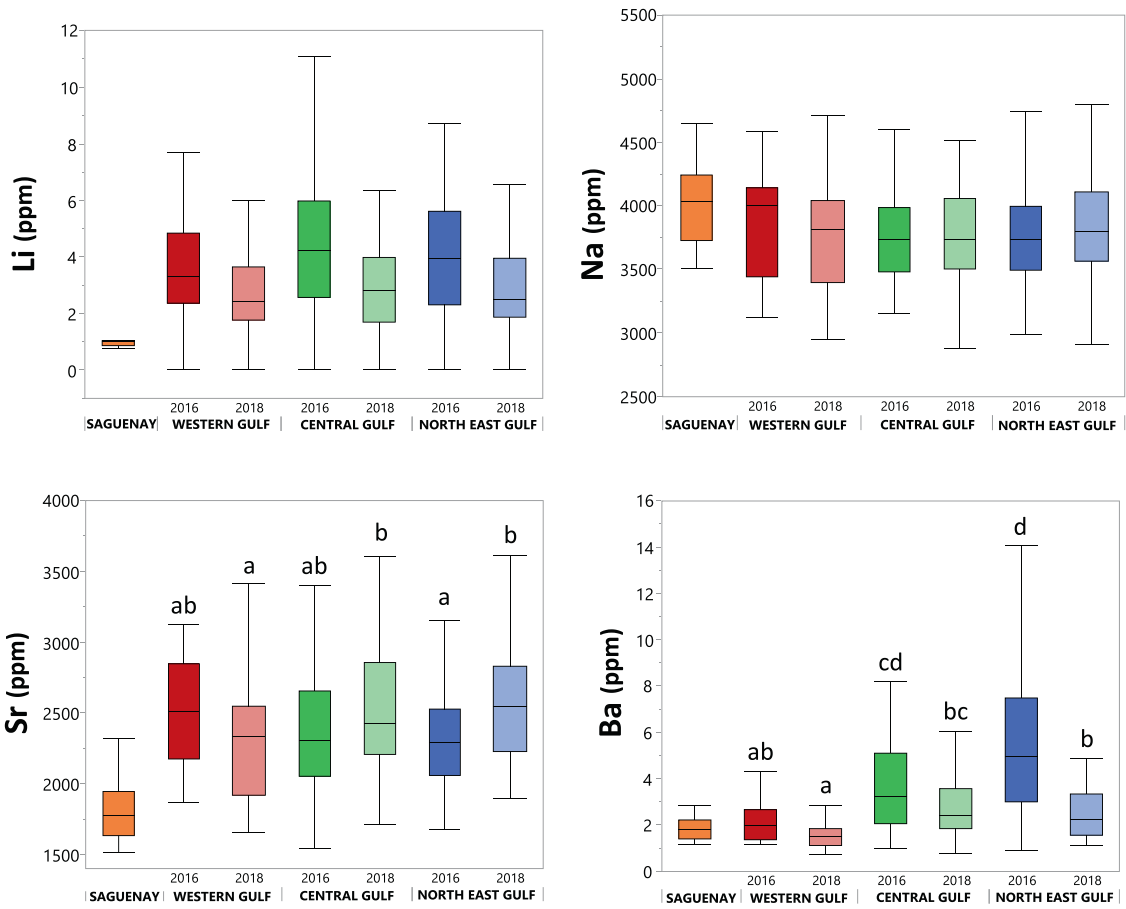


Fig. 4. Boxplot of Li, Na, Sr and Ba concentrations (ppm) measured in otolith edge of redfish by sampling year and sector. The median is represented by the solid line inside of the box representing the interquartile range (IQR). The IQR consist of 50 % of the distribution and the whiskers extend 1.5 times the IQR from the top and bottom of the box. Letters showed significant differences from Tukey's HSD tests following the two-way ANOVA for single element examining temporal (Year), spatial (Sector), and interaction (Year x Sector) variation of elemental concentrations. The ANOVA was performed for GSL individuals exclusively, as individuals from the Saguenay Fjord were only sampled in one year.

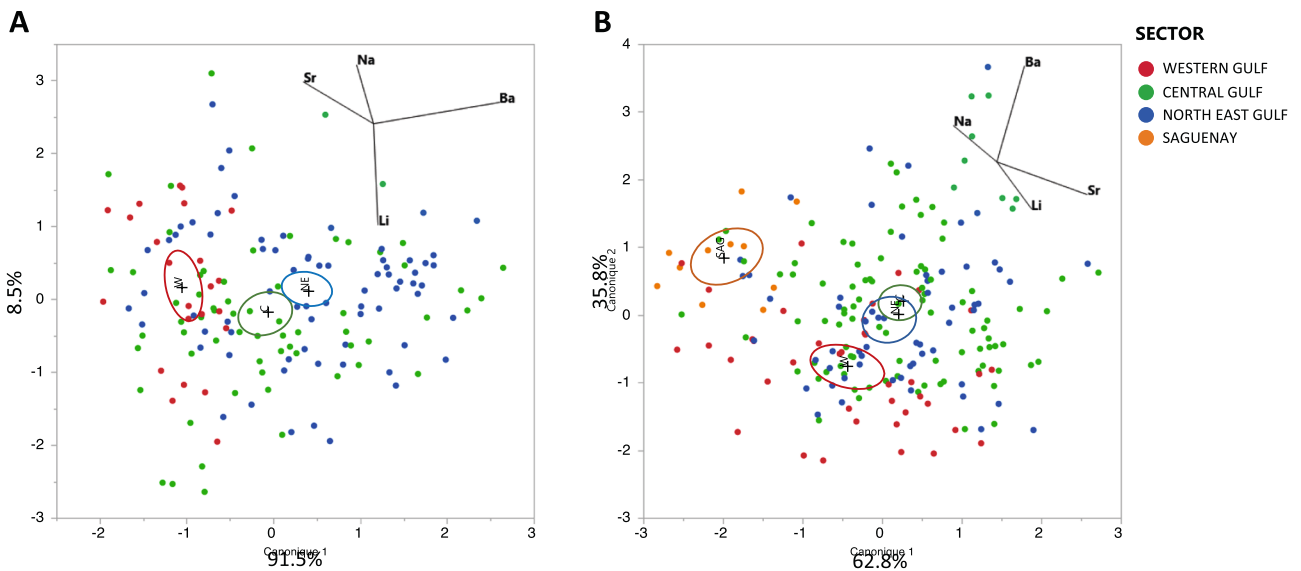


Fig. 5. Quadratic discriminant function analysis (QDFA) based on Li, Na, Sr and Ba concentrations measured in otolith edge of redfish juveniles sampled in (A) 2016 in the GSL and in (B) 2018 in the GSL and the Saguenay Fjord. Each point represents an individual with sampling sectors identified with different colors. Crosses represent the centroids for each sector and ellipses encompasses the 95 % confidence interval of the mean of the groups.

Table 4

Classification results from QDFA per year of sampling based on Li, Na, Sr and Ba concentrations measured in otolith edge of redfish sampled in three sectors of the GSL and in the Saguenay Fjord. Percentage of correctly classified individuals to their collection sector are indicated in bold.

Year	Collection sector	Classification sector				Overall accuracy %
		SAGUENAY	WESTERN GULF	CENTRAL GULF	NORTH EAST GULF	
2016	WESTERN GULF		96	4	0	61
	CENTRAL GULF		31	42	27	
	NORTH EAST GULF		17	16	67	
2018	SAGUENAY	100	0	0	0	48
	WESTERN GULF	2	79	5	14	
	CENTRAL GULF	2	41	37	20	
	NORTH EAST GULF	0	43	24	33	

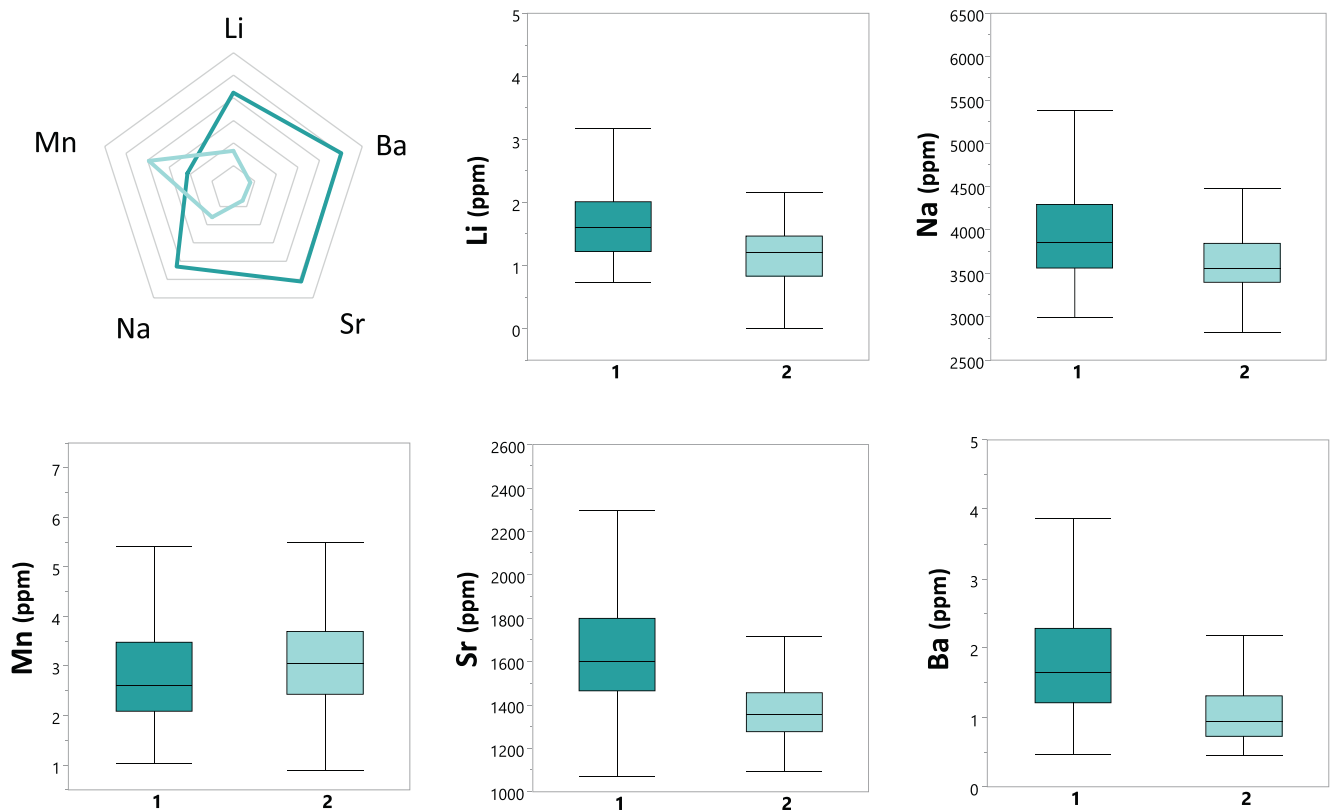


Fig. 6. Radar plot and boxplot of source-specific otolith concentrations (ppm) in Li, Na, Mn, Sr and Ba. Natal sources are referred as source 1 and source 2. Data were standardized to address different elemental concentration units in the radar plot representation.

in the four study sectors, although their contributions varied between eastern and western sectors (Fig. 7). For each cohort, the same East-West distinction was observed in the contribution of the sources (Supplementary Table S1). Source 2 was the main contributor in the Saguenay Fjord, with low presence of source 1 at this location (80.8 % against 18.2 %). For the GSL sectors, the contribution of source 1 increased eastward, from the Western Gulf sector to the North East Gulf sector.

4. Discussion

The potential of otoliths to be used as natural tags for assessing connectivity processes depends on the discriminating power of their chemical signature in the studied system. We estimated the spatial variability in otolith edge fingerprint in the Gulf of St. Lawrence (GSL) and examined the relation between elemental concentrations with

environmental parameters. We found evidence of temporal variability in elemental concentrations more likely attributable to ontogenetic variations (i.e., age- and/or growth-related) than to a change in environmental conditions between the two years of sampling. Otolith core analysis revealed the existence of two possible natal sources contributing to *S. mentella* population from the GSL. The two sources supplied the entire distribution of post-settled juvenile redfish, but their contribution varied between the western and eastern sectors of the GSL. The presumed GSL origin of the sources is discussed in the light of the current information on Northwest Atlantic redfish population structure based on genomics.

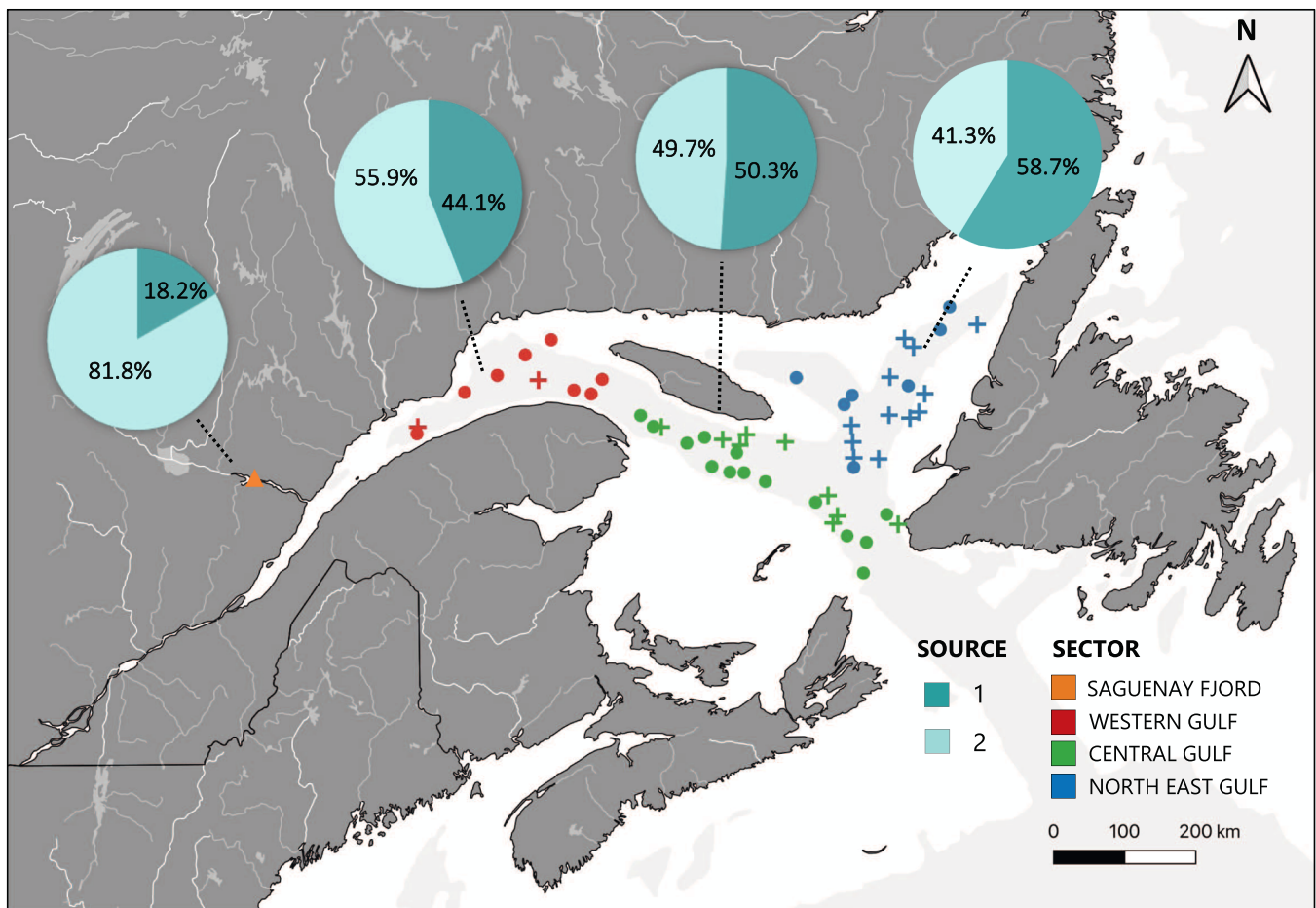


Fig. 7. Pie charts representing the contribution per capture sector (%) of the two natal sources identified by unsupervised RF clustering analysis.

4.1. Spatial variability in otolith fingerprint: Discriminating power of otolith chemistry for redfish in the GSL

The ability of otolith chemistry to investigate redfish movements in the GSL was first demonstrated by Campana et al. (2007), who found evidence of seasonal migrations of *S. mentella* individuals by comparing whole-otolith fingerprints among individuals sampled in the same areas during summer and winter. In the present study, we further investigated *S. mentella* population structure and connectivity at higher spatio-temporal resolution. We relied on laser ablation ICP-MS, a technique that allows precise extraction of the elemental fingerprint from the core and the edge of the otolith. Based on our results, the scale of the spatial variability of the fingerprint was estimated at 100–400 km, corresponding to the distance for which the sectors were clearly distinguishable. Otolith edge concentrations of the four elements (Li, Na, Sr and Ba) exhibiting spatial structure were characterized by similar ranges as those reported in previous solution-based ICP-MS studies carried out in the GSL on *S. mentella* (Campana et al., 2007) and Atlantic cod *Gadus morhua* (Campana et al., 2000). Similar otolith elemental concentrations were also found in *S. mentella* from nursery areas of East Greenland (Stransky et al., 2005), although we found slightly higher Sr concentrations in our study (median around 1800 ppm for redfish from East Greenland versus 2200 ppm for redfish from the GSL). The clear distinction of Saguenay Fjord individuals from the QDFA plot suggests different physio-chemical properties of these waters. Mainly originating from the cold intermediate layer of the St. Lawrence Estuary, the deep-water masses of the Saguenay Fjord are clearly distinguishable from those of the GSL (Xie et al., 2012). Individuals inhabiting the Saguenay Fjord were also distinguishable through whole otolith

dissolution analysis, reflecting their isolation from GSL redfish for much of their life (Campana et al., 2007). It is therefore very unlikely that the chemical distinction of Saguenay Fjord redfish sampled in winter would be attributed to seasonal variation in the fingerprint. In the GSL, the spatial discrimination in otolith chemistry appeared to be driven by Ba concentrations, which increased eastward along with increasing dissolved oxygen concentrations. Furthermore, the barium gradient in the Laurentian channel likely extends outside of the GSL down to the continental slope (Campana et al., 2007). Previous research has shown that the concentration of Ba in the otolith can be directly proportional to the Ba present in the ambient water (Bath et al., 2000), originating from the suspended sediments and released by ion exchange (Coffey et al., 1997). Some studies also reported, like we observed in the present study, a possible link between Ba and dissolved oxygen concentration (Mohan et al., 2014). Together with Ba, Sr also contributed to the discriminatory power of otolith chemistry in the GSL, consistent with findings in several other systems characterized by marked environmental gradients (Elsdon and Gillanders, 2004; Reis-Santos et al., 2013; Secor and Rooker, 2000). In the present study, we found a positive relation between otolith edge concentrations of Sr and water temperature and salinity, which both exhibit steep longitudinal and depth gradients within the Estuary and Gulf of St. Lawrence (Galbraith et al., 2020). The presence of (1) marked environmental gradients in the GSL, (2) significant relationship between some elemental concentration and environmental parameters and (3) spatial variability in otolith Ba and Sr indicate that otolith chemistry analysis is relevant for studying connectivity processes in GSL redfish.

4.2. Temporal variability in otolith fingerprint: Effects from intrinsic and extrinsic factors

The importance of assessing the temporal variability in elemental fingerprints relates to the risk of confounding, or masking, spatial variability. Temporal variability has previously been observed at scales ranging from interannual to seasonal (Gillanders, 2002a; Reis-Santos et al., 2012), and was attributed to either extrinsic (i.e., environmental), or intrinsic factors (i.e., physiological, genetic, ontogenetic) influencing elemental incorporation (reviewed by Hüsey et al. (2020)) and possibly interacting together (Barnes and Gillanders, 2013). In the GSL system, extrinsic factors that may account for the observed between-year variability in otolith Li, Ba and Sr concentrations include: a change in water chemistry influenced by dilution, riverine inputs and oceanic water inflowing (Bewers et al., 1974; Yeats, 1993), and/or variation in the cold intermediate water dynamics (Blais et al., 2019; Galbraith et al., 2020). Indirect influence of environmental change on fish metabolism and incorporation of chemical elements into the calcified structure (e.g., through temperature or salinity variation, Barnes and Gillanders, 2013; Elsdon and Gillanders, 2004) could also potentially explain between-year variability. Since the last decade, the GSL has experienced changing environmental conditions attributable to the decrease in proportion of cold, fresh, and oxygen-rich Labrador Current Water (LCW) in favor of the warm and oxygen-depleted Gulf Stream water entering the Laurentian Channel through Cabot Strait (Blais et al., 2019). This circulation change was associated to a temperature increase and a parallel depletion of oxygen saturation within the bottom layer of the GSL where redfish distribute (Blais et al., 2019; Galbraith et al., 2020). The water temperature recorded during redfish sampling was on average 0.14 °C warmer in 2018 compared to 2016. According to the positive relationship found between temperature and Sr concentrations, the general trend of increasing bottom temperature could have led to the statistically significant increase in otolith Sr in the North East Gulf sector. Likewise, the downward trend in dissolved oxygen concentrations was considered a possible explanation for the between-year decrease in Ba concentrations. However, according to laboratory experiments carried out by Miller (2009) on another *Sebastes* species, *S. melanops*, the effect of temperature on otolith incorporation of chemical elements (Ba and Mn) was only detectable with a greater than 6 °C difference. We thus contend that the modest increase in temperature of less than 1 °C in the deep channels of the GSL between 2016 and 2018 would have resulted in a limited effect compared to possible physiological or ontogenetic factors.

In addition to the effect of extrinsic factors, genetic factors, metabolic processes, growth rate, reproduction, feeding behavior and/or diet, are intrinsic determinants that have been shown to influence element incorporation rates (Hüsey et al., 2020; Miller and Hurst, 2020), potentially confounding fish movement and habitat use reconstruction (Izzo et al., 2018). By targeting and following cohorts over two years, our sampling design was focussed on potential ontogenetic (age- and/or growth-related) influence on the observed variation in Li, Sr and Ba concentrations. Lithium in otolith edge showed no significant relationship with any of the environmental parameters, but concentrations were statistically lower in older redfish. We therefore hypothesize that the temporal variation in otolith Li concentrations were more likely related to age and/or growth change on elemental incorporation rather than change in environmental conditions (Thomas et al., 2017). Causes of variation in otolith Sr and Ba concentrations are by far the most widely investigated, with numerous studies pointing to a strong influence of physiological factors on Sr (Brown and Severin, 2009; de Pontual et al., 2003; Grammer et al., 2017), with possible effects of sex, maturity, and reproductive condition (Sturrock et al., 2014).

In strong 2011–2013 year classes of GSL *Sebastes mentella*, L₅₀ was estimated at 18.1 cm for males and 19.2 cm for females (DFO, 2022), which implies that most of the larger and older individuals sampled in 2018 were mature. This change in sexual maturity status should

therefore be considered as a probable cause for the difference in incorporation of Sr detected in the fingerprint between the smaller and younger redfish captured in 2016, and the older and larger individuals captured in 2018.

Another plausible age-related hypothesis explaining Sr variation patterns is the ontogenetic change in redfish distribution towards deeper water (Atkinson, 1984; Gascon, 2003; Senay et al., 2020). The higher Sr concentrations measured in 2018, which would suggest exposure to warmer and saltier water, coincided with a deeper mean distribution of redfish (as estimated by capture depth) in 2018 relative to 2016 (261.42 m in 2018 compared to 249.58 m in 2016). Other groundfish species like the roundnose grenadier or the polar cod are known to exhibit ontogenetic vertical migrations that are reflected in the otolith elemental fingerprint (Bouchard et al., 2015; Régnier et al., 2017). Even though local changes in environmental conditions between 2016 and 2018 cannot be discarded as a potential cause of the between-year variability in otolith fingerprint, we contend that the change in maturity status and the ontogenetic migration towards deeper habitats are the most likely drivers. The relative importance of these two factors however remains unknown.

4.3. Natal origins

Connectivity and natal origin investigations generally rely on assigning juveniles of unknown origin to a chemical baseline established from the larval fingerprint of individuals collected from known spawning/nursery grounds (Gillanders, 2002b; Thresher, 1999). Since chemical tags are very unlikely to remain stable over years, it is recommended that assignments should be cohort specific (Gillanders, 2002a; Elsdon et al., 2008), making it even more challenging to estimate connectivity processes in slow-growing and long-lived species like redfish. The unsupervised random forest clustering technique represents an alternative approach suitable for studying connectivity in slow-growing fish species in the absence of chemical baseline (Régnier et al., 2017). In the present study, we relied on this clustering analysis of the otolith core fingerprint to characterize the natal sources contributing to the redfish population from the GSL. The significant spatial variability found in otolith edge fingerprint confirmed that the environmental heterogeneity in the GSL system should also be reflected in the otolith core fingerprint. Distinct core fingerprints were then assumed to depict differences in physio-chemical properties of geographically distinct natal sources from which redfish larvae originated. Two natal sources were identified for redfish in the GSL. The possibility that additional sources with overlapping fingerprint may also have contributed however cannot be excluded.

Both sources were present at every sampling sector although they were found in different proportions, yielding information on connectivity between larval and juvenile habitats. The almost exclusive contribution of source 2 to the Saguenay Fjord suggests that individuals inhabiting the Fjord originate from a constrained area. We however reject the hypothesis that the Saguenay Fjord constitutes a source because recently extruded larvae have been shown to not survive longer than few days in the brackish and warm surface waters of the Fjord (Sirois et al., 2009). The Saguenay Fjord is rather considered a sink for marine fish populations of the GSL, including the redfish. Based on the detailed genomic structure of *Sebastes* spp. stocks from the Northwest Atlantic (Benestan et al., 2020), the two identified sources most likely originate from the GSL rather than outside of the system. These authors demonstrated that *S. mentella* individuals from the strong 2011 cohort sampled in the GSL correspond to a single ecotype referred as the GSL ecotype, which highlights the partially isolated nature of the species in the GSL region. When looking at the elemental concentrations characterizing each source, the higher concentrations of Ba and Sr in otolith cores from source 1 individuals were typical of the relatively warmer, saltier, and less hypoxic waters from eastern GSL. In contrast, source 2, which mainly contributed to the western sectors, was characterized by

lower Sr and Ba concentrations, typical of the less saline and more hypoxic waters from the St. Lawrence Estuary. We thus hypothesize that source 1 is located in the Eastern part of the GSL, and source 2 in the Western part. Knowledge available on larval redfish distribution and abundance comes from ichthyoplankton surveys carried out in the 1990s (Sévigny et al., 2000; de Lafontaine, 1990). *S. mentella* larvae were most abundant in the central portion of the Laurentian channel and southeast of Anticosti Island, which would correspond to the hypothesized source 1 located in the Eastern GSL. Recently extruded larvae were also found in waters west of Anticosti Island (Sévigny et al., 2000), an area that could correspond to the location of source 2. The respective dominance of source 1 (of hypothesized Eastern GSL origin) and source 2 (of hypothesized Western GSL origin) in the Eastern and Western sectors of the GSL suggests that redfish juveniles have settled in areas relatively close from where they originated. Evidence of limited larval dispersal has previously been reported in other redfish species along the coasts of Oregon (*Sebastes astrovirens*; (Miller and Shanks, 2004) and California (*Sebastes melanops*; (Standish et al., 2011)). A synoptic ichthyoplankton survey covering all deep channels of the GSL and targeting the *S. mentella* larval extrusion period would help further refining our knowledge of natal source locations.

The present study revealed (1) a significant relationship between otolith elemental concentration and environmental parameters (temperature, dissolved oxygen, salinity and depth); and (2) spatial variability in elemental concentrations in the GSL system, which supports the relevance of otolith chemistry analysis for estimating connectivity processes in GSL *S. mentella*. The identification of an ontogenic shift in otolith elemental concentrations however requires further investigation to disentangle the respective importance of the changing depth habitat with age, and potential habitat-independent age- and/or maturity-related variability in elemental uptake. The potential of using variation in certain chemical elements as an indicator of the onset of maturity should thus be further explored. Our results demonstrated the interest of using unsupervised random forest clustering analysis to estimate connectivity processes in slow-growing and long-lived species that are constrained by temporal variability in the fingerprint. The combination of our otolith chemistry derived results and those based on genomics (Benestan et al., 2020) further improved our understanding of redfish population structure by suggesting that redfish captured in the GSL systematically originate from that region. This emphasizes the advantage of developing holistic approaches integrating multiple natural markers for a robust assessment of stock or population structure (Begg and Waldman, 1999). A logical next step to the present study will be to confirm our hypothesis of limited dispersal of redfish by analysing the entire otolith profile and characterize movements of individuals at finer temporal resolution throughout the early ontogeny.

CRedit authorship contribution statement

DR, PS and LC conceived the project objectives and methodology. LC performed the laboratory processing, operated the LA-ICP-MS analysis, conducted the data analyses, and wrote the first draft of the manuscript. All authors have contributed to the revision and improvements of the manuscript and take responsibility for its content.

Declaration of Competing Interest

The authors declare that they have no known competing financial interests or personal relationships that could have appeared to influence the work reported in this paper.

Data availability

Data will be made available on request.

Acknowledgments

This project was co-funded by Fisheries and Oceans Canada (DFO) and Ressources Aquatiques Québec (RAQ) as part of the partnership program "Return of Groundfish in the Estuary and Northern Gulf of St. Lawrence" supported by the Fonds de recherche du Québec – Nature et technologies (FRQNT), under the leadership of C. Audet from Université du Québec à Rimouski (UQAR). The authors acknowledge all participants in redfish sampling and otolith collection. We want to thank D. Savard and A. Lavoie from LabMaTer, Université du Québec à Chicoutimi (UQAC) for their assistance during the LA-ICP-MS analysis. We are grateful to S. Gagné (UQAC) for help in age reading, A.-L. Fortin (UQAC) for technical assistance, and I. Allie (UQAC) for help in otolith sample preparation. We also want to thank C. Senay and two anonymous reviewers for their helpful suggestions on earlier drafts of the manuscript. D.R. received support from the Canada Research Chairs program.

Appendix A. Supporting information

Supplementary data associated with this article can be found in the online version at doi:10.1016/j.fishres.2023.106739.

References

- Artetxe-Arrate, I., Fraile, I., Crook, D.A., Zudaire, I., Arrizabalaga, H., Greig, A., Murua, H., 2019. Otolith microchemistry: a useful tool for investigating stock structure of yellowfin tuna (*Thunnus albacares*) in the Indian Ocean. *Mar. Freshw. Res.* 70, 1708–1721. <https://doi.org/10.1071/MF19067>.
- Atkinson, D.B., 1984. Distribution and abundance of beaked redfish in the Gulf of St. Lawrence, 1976–81. *J. Northwest Atl. Fish. Sci.* 5, 189–197. <https://doi.org/10.2960/j.v5.a23>.
- Barnes, T.C., Gillanders, B.M., 2013. Combined effects of extrinsic and intrinsic factors on otolith chemistry: implications for environmental reconstructions. *Can. J. Fish. Aquat. Sci.* 70, 1159–1166. <https://doi.org/10.1139/cjfas-2012-0442>.
- Bath, G.E., Thorrold, S.R., Jones, C.M., Campana, S.E., McLaren, J.W., Lam, J.W.H., 2000. Strontium and barium uptake in aragonitic otoliths of marine fish. *Geochim. Cosmochim. Acta* 64, 1705–1714. [https://doi.org/10.1016/S0016-7037\(99\)00419-6](https://doi.org/10.1016/S0016-7037(99)00419-6).
- Begg, G.A., Waldman, J.R., 1999. An holistic approach to fish stock identification. *Fish. Res.* 43, 35–44. [https://doi.org/10.1016/S0165-7836\(99\)00065-X](https://doi.org/10.1016/S0165-7836(99)00065-X).
- Benestan, L.M., Rougemont, Q., Senay, C., Normandeau, E., Parent, E., Rideout, R., Bernatchez, L., Lambert, Y., Audet, C., Parent, G.J., 2020. Population genomics and history of speciation reveal fishery management gaps in two related redfish species (*Sebastes mentella* and *Sebastes fasciatus*). *Evolut. Appl.* 1–19. <https://doi.org/10.1111/eva.13143>.
- Bewers, J.M., Macaulay, I.D., Sundby, B., 1974. Trace metals in the waters of the gulf of St. Lawrence. *Can. J. Earth Sci.* 11, 939–950. <https://doi.org/10.1139/e74-092>.
- Blais, M., Galbraith, P.S., Plourde, S., Scarratt, M., Devine, L., Lehoux, C., 2019. Chemical and biological oceanographic conditions in the estuary and gulf of St. Lawrence during 2018. *Can. Sci. Adv. Sec. Res. Doc.* 2019./059, iv + 64 pp.
- Block, B.A., Teo, S.L.H., Walli, A., Boustany, A., Stokesbury, M.J.W., Farwell, C.J., Weng, K.C., Dewar, H., Williams, T.D., 2005. Electronic tagging and population structure of Atlantic bluefin tuna. *Nature* 434, 1121–1127. <https://doi.org/10.1038/nature03463>.
- Bouchard, C., Thorrold, S.R., Fortier, L., 2015. Spatial segregation, dispersion and migration in early stages of polar cod *Boreogadus saida* revealed by otolith chemistry. *Mar. Biol.* 162, 855–868. <https://doi.org/10.1007/s00227-015-2629-5>.
- Breiman, L., Cutler, A., 2003. Random forests manual v4.0, in: Technical Report. UC Berkeley. (<ftp://ftp.stat.berkeley.edu/pub/users/breiman/Usingrandomforests.v4.0.pdf>).
- Brock, G., Pihur, V., Datta, Susmita, Datta, Somnath, 2008. clValid: an R package for cluster validation. *J. Stat. Softw.* 25, 1–22. <https://doi.org/10.18637/jss.v025.i04>.
- Brown, R.J., Severin, K.P., 2009. Otolith chemistry analyses indicate that water Sr:Ca is the primary factor influencing otolith Sr:Ca for freshwater and diadromous fish but not for marine fish 1808, 1790–1808. <https://doi.org/10.1139/F09-112>.
- Cadrin, S.X., Bernreuther, M., Daniëlsdóttir, A.K., Hjørleifsson, E., Johansen, T., Kerr, L., Kristinsson, K., Mariani, S., Nedreaas, K., Pampoulie, C., Planque, B., Reinert, J., Saborido-Rey, F., Sigurdsson, T., Stransky, C., 2010. Population structure of beaked redfish, *Sebastes mentella*: evidence of divergence associated with different habitats. *ICES J. Mar. Sci.* 67, 1617–1630. <https://doi.org/10.1093/icesjms/fsq046>.
- Campana, S.E., 1999. Chemistry and composition of fish otoliths: pathways, mechanisms and applications. *Mar. Ecol. Prog. Ser.* 188, 263–297. <https://doi.org/10.3354/meps188263>.
- Campana, S.E., Neilson, J.D., 1985. Microstructure of fish otoliths. *Can. J. Fish. Aquat. Sci.* 42, 1014–1032. <https://doi.org/10.1139/f85-127>.
- Campana, S.E., Zwaneburg, K.C.T., Smith, J.N., 1990. ²¹⁰Pb/²²⁶Ra determination of longevity in redfish. *Can. J. Fish. Aquat. Sci.* 47, 163–165. <https://doi.org/10.1139/f90-017>.

- Campana, S.E., Chouinard, G.A., Hanson, J.M., Fréchet, A., Bratley, J., 2000. Otolith elemental fingerprints as biological tracers of fish stocks. *Fish. Res.* 46, 343–357. [https://doi.org/10.1016/S0165-7836\(00\)00158-2](https://doi.org/10.1016/S0165-7836(00)00158-2).
- Campana, S.E., Valentin, A., Sévigny, J.M., Power, D., 2007. Tracking seasonal migrations of redfish (*Sebastes* spp.) in and around the Gulf of St. Lawrence using otolith elemental fingerprints. *Can. J. Fish. Aquat. Sci.* 64, 6–18. <https://doi.org/10.1139/F06-162>.
- Campana, S.E., Valentin, A.E., MacLellan, S.E., Groot, J.B., 2016. Image-enhanced burnt otoliths, bomb radiocarbon and the growth dynamics of redfish (*Sebastes mentella* and *S. fasciatus*) off the eastern coast of Canada. *Mar. Freshw. Res.* 67, 925–936. <https://doi.org/10.1071/MF15002>.
- Chen, L., Liu, Y., Hu, Z., Gao, S., Zong, K., Chen, H., 2011. Accurate determinations of fifty-four major and trace elements in carbonate by LA-ICP-MS using normalization strategy of bulk components as 100%. *Chem. Geol.* 284, 283–295. <https://doi.org/10.1016/j.chemgeo.2011.03.007>.
- Clarke, L.M., Thorrold, S.R., Conover, D.O., 2011. Population differences in otolith chemistry have a genetic basis in *Menidia menidia*. *Can. J. Fish. Aquat. Sci.* 68, 105–114. <https://doi.org/10.1139/F10-147>.
- Coffey, M., Dehairs, F., Collette, O., Luther, G., Church, T., Jickells, T., 1997. The behaviour of dissolved barium in estuaries. *Estuar., Coast. Shelf Sci.* 45, 113–121. <https://doi.org/10.1006/ecss.1996.0157>.
- Cooke, S.J., Midwood, J.D., Thiem, J.D., Klimley, P., Lucas, M.C., Thorstad, E.B., Eiler, J., Holbrook, C., Ebner, B.C., 2013. Tracking animals in freshwater with electronic tags: Past, present and future. *Anim. Biotelemetry* 1, 1–19. <https://doi.org/10.1186/2050-3385-1-5>.
- Cossa, D., Poulet, S.A., 1978. Survey of trace metal contents of suspended matter in the St. Lawrence Estuary and Saguenay Fjord. *J. Fish. Board Can.* 35, 338–345. <https://doi.org/10.1139/f78-060>.
- Cowen, R.K., Sponaugle, S., 2009. Larval dispersal and marine population connectivity. *Annu. Rev. Mar. Sci.* 1, 443–466. <https://doi.org/10.1146/annurev.marine.010908.163757>.
- Cowen, R.K., Gawarkiewicz, G., Pineda, J., Thorrold, S.R., Werner, F.E., 2007. Population connectivity in marine systems: an overview. *Oceanography* 20, 14–21. <https://doi.org/10.5670/oceanog.2007.26>.
- DFO 2022. Redfish (*Sebastes mentella* and *Sebastes fasciatus*) Stocks Assessment in Units 1 and 2 in 2021. DFO Can. Sci. Adv. Sec. Sci. Adv. Rep. 2022/039.
- Eldson, T., Wells, B., Campana, S., Gillanders, B., Jones, C., Limburg, K., Secor, D., Thorrold, S., Walther, B., 2008. Otolith chemistry to describe movements and life-history parameters of fishes: hypotheses, assumptions, limitations and inferences. *Oceanogr. Mar. Biol.: Annu. Rev.* 46, 297–330. <https://doi.org/10.1201/9781420065756.ch7>.
- Eldson, T.S., Gillanders, B.M., 2004. Fish otolith chemistry influenced by exposure to multiple environmental variables. *J. Exp. Mar. Biol. Ecol.* 313, 269–284. <https://doi.org/10.1016/j.jembe.2004.08.010>.
- Galbraith, P.S., Chassé, J., Shaw, J.-L., Dumas, J., Caverhill, C., Lefavre, D., Lafleur, C., 2020. Physical oceanographic conditions in the gulf of St. Lawrence during 2019. *DFO Can. Sci. Adv. Sec. Res. Doc.* 2020/30, iv + 88 pp.
- , 2003Gascon, D. (ed.) 2003. Redfish Multidisciplinary Research Zonal Program (1995–1998): Final Report. Can. Tech. Rep. Fish. Aquat. Sci. 2462: xiii + 139 p.
- Gibb, F.M., Régner, T., Donald, K., Wright, P.J., 2017. Connectivity in the early life history of sandeel inferred from otolith microchemistry. *J. Sea Res.* 119, 8–16. <https://doi.org/10.1016/j.seares.2016.10.003>.
- Gillanders, B.M., 2002a. Temporal and spatial variability in elemental composition of otoliths: Implications for determining stock identity and connectivity of populations. *Can. J. Fish. Aquat. Sci.* 59, 669–679. <https://doi.org/10.1139/f02-040>.
- Gillanders, B.M., 2002b. Connectivity between juvenile and adult fish populations: do adults remain near their recruitment estuaries? *Mar. Ecol. Prog. Ser.* 240, 215–223. <https://doi.org/10.3354/meps240215>.
- Grammer, G.L., Morrongiello, J.R., Izzo, C., Hawthorne, P.J., Middleton, J.F., Gillanders, B.M., 2017. Coupling biogeochemical tracers with fish growth reveals physiological and environmental controls on otolith chemistry. *Ecol. Monogr.* 87, 487–507. <https://doi.org/10.1002/ecm.1264>.
- Hüssy, K., Limburg, K.E., Pontual, H., De, Thomas, O.R.B., Cook, K., Heimbrand, Y., Blass, M., Sturrock, A.M., Hüssy, K., Limburg, K.E., Pontual, H., De, Thomas, O.R.B., 2020. Trace element patterns in otoliths: The role of biomineralization trace element patterns in otoliths: the role of biomineralization. *Rev. Fish. Sci. Aquac.* 0, 1–33. <https://doi.org/10.1080/23308249.2020.1760204>.
- Izzo, C., Reis-Santos, P., Gillanders, B.M., 2018. Otolith chemistry does not just reflect environmental conditions: a meta-analytic evaluation. *Fish. Fish.* 19, 441–454. <https://doi.org/10.1111/faf.12264>.
- Jarvis, E.T., Lowe, C.G., 2008. The effects of barotrauma on the catch-and-release survival of southern California nearshore and shelf rockfish (*Scorpaenidae*, *Sebastes* spp.). *Can. J. Fish. Aquat. Sci.* 65, 1286–1296. <https://doi.org/10.1139/F08-071>.
- Kaufman, L., Rousseeuw, P.J., 1990. Finding Groups in Data: An Introduction to Cluster Analysis. Wiley Series in Probability and Mathematical Statistics. John Wiley & Sons, New York. <https://doi.org/10.1002/9780470316801>.
- Kerr, L.A., Campana, S.E., 2014. Chemical composition of fish hard parts as a natural marker of fish stocks. In: Cadrin, S.X., Kerr, L.A., Mariani, S. (Eds.), *Stock Identification Methods*, second ed. Academic Press, San Diego, pp. 205–234. <https://doi.org/10.1016/B978-0-12-397003-9.00011-4>.
- Koutitonsky V.G. and Bugden G.L. 1991. The physical oceanography of the Gulf of St. Lawrence: a review with emphasis on the synoptic variability of the motion. In: Theriault J.-C. (Ed.), *The Gulf of St. Lawrence: Small Ocean or Big Estuary?* Canadian Special Publication of Fisheries and Aquatic Sciences, 113: 57–90.
- de Lafontaine, Y., 1990. Ichthyoplankton communities in the St. Lawrence Estuary: composition and dynamics. In: El-Sabh, M.I., Silverberg, N. (Eds.), *Oceanography of a Large-Scale Estuarine System: The St. Lawrence*. Springer-Verlag, New York, pp. 321–343. https://doi.org/10.1007/978-1-4615-7534-4_14.
- Lazartigues, A.V., Sirois, P., Savard, D., 2014. LA-ICP-MS analysis of small samples: carbonate reference materials and larval fish otoliths. *Geostand. Geoanal. Res.* 38, 225–240. <https://doi.org/10.1111/j.1751-908X.2013.00248.x>.
- Leaman, B.M., Nagtegaal, D.A., 1987. Age validation and revised natural mortality rate for yellowtail rockfish. *Trans. Am. Fish. Soc.* 116, 171–175. [https://doi.org/10.1577/1548-8659\(1987\)116<171:avarmn>2.0.co;2](https://doi.org/10.1577/1548-8659(1987)116<171:avarmn>2.0.co;2).
- Mayo, R.K., Gifford, V.M., Jearld Jr., A., 1981. Age validation of Redfish, *Sebastes marinus* (L.), from the Gulf of Maine-Georges bank region. *J. Northwest Atl. Fish. Sci.* 2, 13–19. <https://doi.org/10.2960/J.v2.a2>.
- Miller, J.A., 2009. The effects of temperature and water concentration on the otolith incorporation of barium and manganese in black rockfish *Sebastes melanops*. *J. Fish. Biol.* 75, 39–60. <https://doi.org/10.1111/j.1095-8649.2009.02262.x>.
- Miller, J.A., Hurst, T.P., 2020. Growth rate, ration, and temperature effects on otolith elemental incorporation. *Front. Mar. Sci.* 7, 1–16. <https://doi.org/10.3389/fmars.2020.00320>.
- Miller, J.A., Shanks, A.L., 2004. Evidence for limited larval dispersal in black rockfish (*Sebastes melanops*): implications for population structure and marine-reserve design. *Can. J. Fish. Aquat. Sci.* 61, 1723–1735. <https://doi.org/10.1139/F04-111>.
- Mohan, J., Rahman, M.S., Thomas, P., Walther, B., 2014. Influence of constant and periodic experimental hypoxic stress on Atlantic croaker otolith chemistry. *Aquat. Biol.* 20, 1–11. <https://doi.org/10.3354/ab00542>.
- Morisette, O., Sirois, P., 2021. Flowing down the river: Influence of hydrology on scale and accuracy of elemental composition classification in a large fluvial ecosystem. *Sci. Total Environ.* 760, 143320. <https://doi.org/10.1016/j.scitotenv.2020.143320>.
- Nedreaas, K., 1990. Age determination of Northeast Atlantic *Sebastes* species. *J. du Cons. Int. pour l'Exploitation De. la Mer.* 47, 208–230. <https://doi.org/10.1093/icesjms/47.2.208>.
- Norse, E.A., Brooke, S., Cheung, W.W.L., Clark, M.R., Ekeland, I., Froese, R., Gjerde, K. M., Haedrich, R.L., Heppell, S.S., Morato, T., Morgan, L.E., Pauly, D., Sumaila, R., Watson, R., 2012. Sustainability of deep-sea fisheries. *Mar. Policy* 36, 307–320. <https://doi.org/10.1016/j.marpol.2011.06.008>.
- Pan, X., Ye, Z., Xu, B., Jiang, T., Yang, J., Tian, Y., 2020. Population connectivity in a highly migratory fish, Japanese Spanish mackerel (*Scomberomorus niphonius*), along the Chinese coast, implications from otolith chemistry. *Fish. Res.* 231, 105690. <https://doi.org/10.1016/j.fishres.2020.105690>.
- Paton, C., Hellstrom, J., Paul, B., Woodhead, J., Hergt, J., 2011. Iolite: freeware for the visualisation and processing of mass spectrometric data. *J. Anal. At. Spectrom.* 26, 2508–2518. <https://doi.org/10.1039/c1ja10172b>.
- de Pontual, H., Lagardère, F., Amara, R., Bohn, M., Ogor, A., 2003. Influence of ontogenetic and environmental changes in the otolith microchemistry of juvenile sole (*Solea solea*). *J. Sea Res.* 50, 199–211. [https://doi.org/10.1016/S1385-1101\(03\)00080-7](https://doi.org/10.1016/S1385-1101(03)00080-7).
- Quinn, G.P., Keough, M.J., 2002. *Experimental Design and Data Analysis for Biologists*. Cambridge University Press.
- Régner, T., Augley, J., Devalla, S., Robinson, C.D., Wright, P.J., Neat, F.C., 2017. Otolith chemistry reveals seamont fidelity in a deepwater fish. *Deep-Sea Res. Part I: Oceanogr. Res. Pap.* 121 183–189. <https://doi.org/10.1016/j.dsr.2017.01.010>.
- Reis-Santos, P., Gillanders, B.M., Tanner, S.E., Vasconcelos, R.P., Eldson, T.S., Cabral, H. N., 2012. Temporal variability in estuarine fish otolith elemental fingerprints: implications for connectivity assessments. *Estuar., Coast. Shelf Sci.* 112, 216–224. <https://doi.org/10.1016/j.ecss.2012.07.027>.
- Reis-Santos, P., Tanner, S.E., Vasconcelos, R.P., Eldson, T.S., Cabral, H.N., Gillanders, B. M., 2013. Connectivity between estuarine and coastal fish populations: contributions of estuaries are not consistent over time. *Mar. Ecol. Prog. Ser.* 491, 177–186. <https://doi.org/10.3354/meps10458>.
- Saha, A., Johansen, T., Hedeholm, R., Nielsen, E.E., Westgaard, J.I., Hauser, L., Planque, B., Cadrin, S.X., Boje, J., 2017. Geographic extent of introgression in *Sebastes mentella* and its effect on genetic population structure. *Evolut. Appl.* 10, 77–90. <https://doi.org/10.1111/eva.12429>.
- Schafer, C.T., Smith, J.N., Côté, R., 1990. The Saguenay Fjord: a major tributary to the St. Lawrence estuary. In: El-Sabh, M.I., Silverberg, N. (Eds.), *Oceanography of a Large-scale Estuarine System*. Springer, St. Lawrence, pp. 378–420.
- Secor, D.H., 2015. *Migration Ecology of Marine Fishes*. Johns Hopkins University Press, Baltimore.
- Secor, D.H., Rooker, J.R., 2000. Is otolith strontium a useful scalar of life cycles in estuarine fishes. *Fish. Res.* 46, 359–371. [https://doi.org/10.1016/S0165-7836\(00\)00159-4](https://doi.org/10.1016/S0165-7836(00)00159-4).
- Senay, C., Ouellette-plante, J., Bourdages, H., Birmingham, T., Parent, G., Chabot, D., Duplisa, D., 2020. Unit 1 Redfish (*Sebastes mentella* and *S. fasciatus*) stock status in 2019 and updated information on population structure, biology, ecology, and current fishery closures.
- Sévigny, J.M., Gagné, P., De Lafontaine, Y., Dodson, J., 2000. Identification and distribution of larvae of redfish (*Sebastes fasciatus* and *S. mentella*: Scorpaenidae) in the Gulf of St. Lawrence. *Fish. Bull.* 98, 375–388.
- Sévigny, J.-M., Valentin, A., Talbot, A., Ménard, N., 2009. Connectivité entre les populations du Fjord du Saguenay et celles du golfe du Saint-Laurent. *Rev. Des. Sci. De. l'eau* 22, 315–339. <https://doi.org/10.7202/037487ar>.
- Shi, T., Horvath, S., 2006. Unsupervised learning with random forest predictors. *J. Comput. Graph. Stat.* 15 (1), 118–138. <https://doi.org/10.1198/106186006x94072>.
- Sigurdsson, T., Thorsteinsson, V., Gústafsson, L., 2006. In situ tagging of deep-sea redfish: application of an underwater, fish-tagging system. *ICES J. Mar. Sci.* 63, 523–531. <https://doi.org/10.1016/j.icesjms.2005.05.023>.

- Sirois, P., Diab, G., Fortin, A.-L., Plourde, S., Gagné, J.A., Ménard, N., 2009. Recrutement des poissons dans le fjord du Saguenay. *Rev. Des. Sci. De. l'eau / J. Water Sci.* 22 (2), 341–352. <https://doi.org/10.7202/037488ar>.
- Standish, J.D., White, J.W., Warner, R.R., 2011. Spatial pattern of natal signatures in the otoliths of juvenile kelp rockfish along the Californian coast. *Mar. Ecol. Prog. Ser.* 437, 279–290. <https://doi.org/10.3354/meps09241>.
- Stransky, C., Garbe-Schönberg, C.D., Günther, D., 2005. Geographic variation and juvenile migration in Atlantic redfish inferred from otolith microchemistry. *Mar. Freshw. Res.* 56, 677–691. <https://doi.org/10.1071/MF04153>.
- Sturrock, A.M., Trueman, C.N., Darnaude, A.M., Hunter, E., 2012. Can otolith elemental chemistry retrospectively track migrations in fully marine fishes, 44, 766–795. <https://doi.org/10.1111/j.1095-8649.2012.03372.x>.
- Sturrock, A.M., Trueman, C.N., Milton, J.A., Waring, C.P., Cooper, M.J., Hunter, E., 2014. Physiological influences can outweigh environmental signals in otolith microchemistry research. *Mar. Ecol. Prog. Ser.* 500, 245–264. <https://doi.org/10.3354/meps10699>.
- Sturrock, A.M., Hunter, E., Milton, J.A., Johnson, R.C., Waring, C.P., Trueman, C.N., EIMF, 2015. Quantifying physiological influences on otolith microchemistry. *Methods Ecol. Evol.* 6, 806–816. <https://doi.org/10.1111/2041-210X.12381>.
- Thomas, O.R.B., Ganio, K., Roberts, B.R., Swearer, S.E., 2017. Trace element-protein interactions in endolymph from the inner ear of fish: implications for environmental reconstructions using fish otolith chemistry. In: *Metallomics: Integrated Biometal Science*, 9. Royal Society of Chemistry, pp. 239–249. <https://doi.org/10.1039/c6mt00189k>.
- Thorrold, S.R., Latkoczy, C., Swart, P.K., Jones, C.M., 2001. Natal homing in a marine fish. *Science* 291 (5502), 297–299. <https://doi.org/10.1126/science.291.5502.29>.
- Thorrold, S.R., Jones, G.P., Hellberg, M.E., Burton, R.S., Swearer, S.E., Neigel, J.E., Morgan, S.G., Warner, R.R., 2002. Quantifying larval retention and connectivity in marine populations with artificial and natural markers. *Bull. Mar. Sci.* 70 ((Suppl.1), 291–308. (<https://escholarship.org/uc/item/5490p10z>).
- Thresher, R.E., 1999. Elemental composition of otoliths as a stock delineator in fishes. *Fish. Res.* 43 (1–3), 165–204. [https://doi.org/10.1016/S0165-7836\(99\)00072-7](https://doi.org/10.1016/S0165-7836(99)00072-7).
- Valentin, A.E., Penin, X., Chanut, J.P., Power, D., Sévigny, J.M., 2014. Combining microsatellites and geometric morphometrics for the study of redfish (*Sebastes* spp.) population structure in the Northwest Atlantic. *Fish. Res.* 154, 102–119. <https://doi.org/10.1016/j.fishres.2014.02.008>.
- Wright, P.J., Régnier, T., Gibb, F.M., Augley, J., Devalla, S., 2018a. Identifying stock structuring in the sandeel, *Ammodytes marinus*, from otolith microchemistry. *Fish. Res.* 199, 19–25. <https://doi.org/10.1016/j.fishres.2017.11.015>.
- Wright, P.J., Régnier, T., Gibb, F.M., Augley, J., Devalla, S., 2018b. Assessing the role of ontogenetic movement in maintaining population structure in fish using otolith microchemistry. *Ecol. Evol.* 17, 7907–7920. <https://doi.org/10.1002/ece3.4186>.
- Xie, H., Aubry, C., Bélanger, S., Song, G., 2012. The dynamics of absorption coefficients of CDOM and particles in the St. Lawrence estuarine system: biogeochemical and physical implications. *Mar. Chem.* 128–129, 44–56. <https://doi.org/10.1016/j.marchem.2011.10.001>.
- Yeats, P.A., 1993. Input of metals to the North Atlantic from two large Canadian estuaries. *Mar. Chem.* 43, 201–209. [https://doi.org/10.1016/0304-4203\(93\)90225-D](https://doi.org/10.1016/0304-4203(93)90225-D).